Published in final edited form as:

Biotechnol Bioeng. 2016 November ; 113(11): 2403–2415. doi:10.1002/bit.26017.

Genome-scale RNA interference screen identifies antizyme 1(OAZ1) as a target for improvement of recombinant protein production in mammalian cells†

Su Xiao[1,2], **Yu Chi Chen**[3], **Eugene Buehler**[3], **Swati Mandal**[4], **Ajeet Mandal**[4], **Michael Betenbaugh**[2], **Myung HeePark**[4], **Scott Martin**[3,*], and **Joseph Shiloach**[1,*]

[1]Biotechnology Core Laboratory NIDDK, NIH Bethesda Maryland 20892, USA

[2]Department of Chemical and Biomolecular engineering Johns Hopkins University, Baltimore Maryland 21218, USA

[3]Chemical Genomics Center, National Center for Advancing Translational Sciences, NIH Rockville MD 20850

[4]Molecular & Cellular Biochemistry Section, NIDCR, NIH. Bethesda MD 20892

Abstract

For the purpose of improving recombinant protein production from mammalian cells, an unbiased, high-throughput whole-genome RNA interference screen was conducted using human embryonic kidney 293 (HEK 293) cells expressing firefly luciferase. 21,585 human genes were individually silenced with three different siRNAs for each gene. The screen identified 56 genes that led to the greatest improvement in luciferase expression. These genes were found to be included in several pathways involved in spliceosome formation and mRNA processing, transcription, metabolic processes, transport and protein folding. The 10 genes that most enhanced protein expression when down regulated, were further confirmed by measuring the effect of their silencing on the expression of three additional recombinant proteins.

Among the confirmed genes, *OAZ1*- the gene encoding the ornithine decarboxylase antizyme1- was selected for detailed investigation, since its silencing improved the reporter protein production without affecting cell viability. Silencing *OAZ1* caused an increase of the ornithine decarboxylase enzyme and the cellular levels of putrescine and spermidine; an indication that increased cellular polyamines enhances luciferase expression without affecting its transcription. The study shows that *OAZ1* is a novel target for improving expression of recombinant proteins. The genome-scale screening performed in this work can establish the foundation for targeted design of an efficient mammalian cell platform for various biotechnological applications.

---

†This article has been accepted for publication and undergone full peer review but has not been through the copyediting, typesetting, pagination and proofreading process, which may lead to differences between this version and the Version of Record. Please cite this article as doi: [10.1002/bit.26017]

*To whom correspondence should be addressed. Tel:(1) 301 496 9719 Fax: (1)301 496 5911 Josephs@nih.gov. Correspondence may also be addressed to Scott Martin.

Present Address: Scott Martin Functional Genomics Genentech Inc. Yu Chi Chen Center for proteome Chemistry Novartis

Additional Supporting Information may be found in the online version of this article.

Keywords

siRNA; HEK 293; OAZ1; Luciferase; protein production

Introduction

RNA interference (RNAi), first discovered as a natural biological process of eukaryotic cells for protecting the genome against foreign nucleic acids (Napoli et al., 1990; van der Krol et al., 1990), has been developed and utilized as a revolutionary tool in deducing gene functions and in combating genetic defects, viral diseases, autoimmune disorders, and cancers (Aagaard and Rossi, 2007). siRNAs are 21–25 nucleotide double-strand RNA fragments with symmetric 2-nucleotides 3'-end overhangs (Hamilton and Baulcombe, 1999). The guide strand of siRNA can be incorporated into RNA-induced silencing complex (RISC), which brings about sequence-specific degradation of the homologous single stranded mRNAs (Jinek and Doudna, 2009). In recent years, large-scale genetic screens have been made possible by the availability of genome-wide siRNA libraries, as well as the development of sophisticated new instrumentation and bioinformatics approaches for data analysis (Conrad and Gerlich, 2010; Huang et al., 2009). They have been used to investigate the biological functions of specific genes and pathways in various diseases (Seyhan and Rya, 2010) and important biological processes, including signal transduction, cell aging or death, cell or organelle organization, protein localization and responses of host cells to pathogens (Bard et al., 2006;.Brognard and Hunter, 2011; Cherry, 2008; Ni and Lee, 2010;Orvedahl et al., 2011). However, there has been limited use of a genome-wide siRNA screen for improving heterologous protein production (Bard et al., 2006; Simpson et al., 2012), an important process intensively investigated by the pharmaceutical and biotechnology industry.

In the current work, we performed a genome-wide siRNA screen to identify genes that may influence recombinant protein production, using *Photinus pyralis* (firefly) luciferase as a reporter protein. With a high-throughput format, 21,585 genes were individually silenced with three different siRNAs, in HEK-CMV-Luc2-Hygro cells constitutively expressing firefly luciferase. The viable cell number and the luciferase activity were measured following the screening and the results were incorporated into genome-wide loss-of-function data. Statistical data analyses were conducted, followed by a validation screen where ten target genes (leading to greatest improvement of luciferase production) were confirmed. Among these selected genes, *OAZ1* the gene that encodes antizyme 1, an inhibitor of ornithine decarboxylase (Pegg, 2006),was chosen for more detailed studies, since its silencing caused minimal effect on cell viability.

Materials and Methods

Cell culture

HEK-CMV-Luc2-Hygro cell line constitutively expressing *P. pyralis* luciferase (Progema) and HEK- GPC3-hFc cell line constitutively secreting glypican-3 hFc-fusion protein (GPC3-hFc)(Feng et al., 2013) (a gift from Dr. Mitchell Ho, NCI, National Institutes of Health)

were maintained in DMEM containing 10% fetal bovine serum (FBS). The inducible T-Rex-SERT-GFP cell line (Abdul-Hussein et al. 2013)and T-Rex-NTSR1-GFP cell line (Xiao et al. 2015) were maintained as an adherent culture in DMEM containing 10% certified FBS, 5μg/mL blasticidin and 200μg/mL zeocin (Invitrogen). All cells were maintained in a humidified incubator set at 37°C and 5% CO_2.

High-throughput genome-wide screen for luciferase expression

The Silencer® Select Human genome siRNA library (Ambion), which targets 21,585 human genes with 3 siRNAs per gene, was used for screening. Each siRNA is arrayed in an individual well (Corning 3570, 384 well, white, solid bottom plates). The transfection was done in duplicates: 0.8 pmol of each siRNA was spotted to a well of a 384-well plate (Corning) and 20 μL of serum-free DMEM containing 0.07 μL of Lipofectamine RNAiMax (Life Technologies) was then added to each well. This lipid-siRNA mixture was incubated at ambient temperature for 30 minutes prior to addition of 4000 cells in 20 μL of DMEM containing 20% FBS (Gibco). After incubating the transfected cells at 37°C in 5% CO_2 for 72 hours, 20 μL of ONE-Glo™ Reagent (Promega) was added to one set of replicates for 'overall luciferase yield' quantification and 20 μL of Cell Titer-Glo™ Reagent (Promega) was added to the second set of replicates for 'viable cell density' measurement. All plates were incubated at room temperature for 20 minutes to stabilize the luminescent signal and the signal was then measured with PerkinElmer Envision 2104 Multilabel plate reader. All plates had a full column (16 wells) of Silencer Select Negative Control #2 (Life Technologies) for data normalization and a full column of *siPLK1* (Ambion Silencer Select, cat# s448) was also used as on-plate reference for transfection efficiency. Both controls were also used in all validation transfections.

The 56 genes which got targeted by at least two independent siRNAs (out of three) resulting in enhanced luciferase production with MAD-based z-score>3 from the primary screen were subjected to validation screen using 3 additional Silencer® siRNAs (Ambion) with different sequences from those used in the primary screen. Ten gene candidates were selected based on the criteria that 3 out of 6 siRNAs displayed a MAD-based z-score>3. The transfection and assay processes were the same as in the primary genome-wide screen. Data visualization was performed in R computational environment (https://www.R-project.org/) by using 'hexbin' and 'ggplot2' packages (R Core Team, 2015; Carr, 2015; Wickham, 2009).

Statistical analysis of primary screen data

The screen generated end-point data for 'overall luciferase yield' and 'viable cell density' in each well. For each plate, the median value of the negative control wells was set as 100% and was used to normalize corresponding sample wells. The 'overall luciferase yield' and 'viable cell density' were exported as % of negative control and the median absolute deviation (MAD) - based z-score was calculated for each sample (Chung et al., 2008).

Gene ontology (GO) analysis

In order to get the maximum coverage of GO annotation data for 119 selected siRNA's targeting 56 genes, PANTHER classification system (http://www.pantherdb.org/) and AmiGO 2 GO browser were used (Mi et al., 2013; Carbon et al., 2009). The construction of

a heat map was accomplished using Partek® Genomics Suite® software, version 6.6 Copyright ©; 2015, Partek Inc., St. Louis, MO, USA.

Validation transfection

Ten targeted genes were selected and tested in four HEK 293 cell lines expressing different reporter proteins, glycan-3 hFc-fusion protein (GPC3-hFc), neurotensin receptor type 1-GFP (NTSR1-GFP) and serotonin transporter-GFP (SERT-GFP), using 1 representative siRNA for each gene. Transfection was performed in 12-well plate format. 500μL of serum-free DMEM media containing siRNA and Lipofectamine RNAiMax was incubated in each well for 20 min at ambient temperature and 500μL DMEM containing 20% FBS and cells was then added for transfection. The final siRNA concentration in each well was 40nM. Lipofectamine RNAiMax volumne and cell seeding number in each well have been optimized for each cell line (Table S1).

ELISA for determination of GPC3-hFc production

5 days after transfection, clarified cell culture supernatant was used for determination of GPC3-hFc concentration by ELISA and cells were detached and counted by trypan blue exclusion using a CEDEX cell quantification system (Roche, Mannheim, Germany). AffiniPure F(ab')$_2$ Fragment Goat Anti-Human IgG (min X Bov, Ms, RbSrProt, Cat. 109-006-170, Jackson Immunology,5μg/mL in PBS) was used to coat a 96-well plate (50 μL per well) at 4°C overnight. After blocking the plate with 2% BSA in PBS, 50μl of pre-diluted cell culture supernatant was added, and the plate was incubated at room temperature for 1 h to allow binding to occur. After the plate was washed twice with PBS containing 0.05% Tween 20, Peroxidase-conjugated AffiniPure Goat-anti-human IgG (Cat. 109-035-098, Jackson Immunology) was added at 1:4000 dilution (50μL/well). Following incubation at room temperature for 1 hour, the plate was washed 4 times and signals were detected with Peroxidase Substrate System (KPL).

Flow cytometry analysis for determination of NTSR1-GFP and SERT-GFP production

3 days after transfection, cells were induced with 1μg/mL tetracycline. 24 hours later, cells from each well were detached with non-enzymatic cell dissociation buffer (Gibco, Cat. No. 13150-016) and washed twice with cold PBS. Cell densities were adjusted to 0.5 million cells/mL with PBS and then subjected to flow cytometry analysis. Green fluorescence was measured with Guava Easycyte 5HT and Incyte software (Millipore). The green fluorescence signal and cell gating were adjusted using uninduced T-REx-293-NTSR1-GFP cells, with more than 99.5% of the cells in low fluorescence range (<100). The setting was kept the same for all cell samples.

OAZ1 silencing studies

HEK-CMV-Luc2-Hygro cells in 6 well plates were transfected with Silencer siRNA for *oaz1* gene (Catalog number: AM51331, assay ID: 46078). The transfection was done in 6-well plate format: 0.12 nmol of each siRNA and 1.5mL of serum-free DMEM containing 11.25 μL of Lipofectamine RNAiMax (Life Technologies) was then added to each well. This lipid-siRNA mixture was incubated at ambient temperature for 30 min prior to adding 2×10^5 cells

in 1.5mL of DMEM containing 20% FBS (Gibco). The transfected cells were incubated at 37°C in 5% CO_2 and were harvested after 24, 48, 72 and 96 hours. Luciferase activity was determined using ONE-Glo™ Reagent (Promega) and aliquots of transfected cells.

Isolation of RNA and real-time qRT-PCR

Cells were trypsinized from 6-well plates, washed twice with cold PBS and cell pellets were flash frozen on dry ice and stored at −80°C until extraction. RNA was extracted using the RNeasy kit (Qiagen) and then treated with DNase using TURBO DNA-free™ Kit (Life Technologies). cDNA was generated from the RNA using the Maxima Frist Strand cDNA Synthesis Kit for qRT-PCR (Thermo Scientific). The real-time qPCR was performed using *Fast SYBR® Green* Master Mix (Life Technologies) in 7900 HT Fast Real Time PCR System (*Applied Biosystems*).The $2^{-\Delta\Delta Ct}$ method was used for relative expression analysis(Livak and Schmittgen, 2001) with *GAPDH* as the reference gene. Cells transfected with negative control siRNA and harvested after 24hours were set as calibrator. Primers used for each gene are: *luc* (Promega), 5'-TCACGAAGGTGTACATGCTTTGG-3' and 5'-GATCCTCAACGTGCAAAAGAAGC-3'; *ODC1*, 5'-TAAAGGAACAGACGGGCTCT-3' and 5'- CCATAGACGCCATCATTCAC-3'; *OAZ1*: 5'- GGAACCGTAGACTCGCTCAT-3' and 5'-TCGGAGTGAGCGTTTATTTG-3'; *GAPDH*: 5'-CATCAATGGAAATCCCATCA-3' and 5'- TTCTCCATGGTGGTGAAGAC-3'.

Western blotting

Transfected cells were lysed in buffer containing 50 mMTris-HCl, pH 7.4, 5 mM EDTA, 150 mM NaCl, 1% Nonidet P-40, and protease inhibitor mixture. Proteins (~20 μg) were separated by SDS-PAGE (4–12% gel) in MES buffer and transferred to 0.2-μm nitrocellulose membrane for immunodetection using mouse anti-ODC (Sigma, catalog number O1136) and mouse anti-β-actin (BD biosciences, catalogue number 612657) primary antibodies and HRP conjugated anti-mouse secondary antibodies (abCAM, catalog number ab20043). Signals were detected with an ECL Plus chemiluminescence reagent.

Measurement of cellular polyamine concentration

Cells in six-well plates were washed twice with PBS, harvested, and precipitated with 0.1mL cold 10% trichloroacetic acid (TCA). A total of 50μL of the TCA supernatant was used for polyamine analysis by an ion exchange chromatographic system (Biochrom). TCA precipitates were dissolved in 0.1 N NaOH and aliquots were used for protein determination by the Bradford method. Polyamine contents were estimated as nmol/mg protein.

Results

1. Identification of genes whose silencing leads to enhanced luciferase expression

A human genome-wide siRNA screen was conducted in HEK-CMV-Luc2-Hygrocells by using siRNA library targeting 21,585 human genes, with 3 independent arrayed siRNAs per gene. The transfection was done in duplicate: one set of plates was used for measuring the overall luciferase yield and the second set was used for the determination of viable cell density, from which the per cell luciferase yield was calculated (Figure 1A). The distribution of siRNA activity based on the overall luciferase yield is illustrated in the histogram shown

in Figure 1B, where the red and blue colour circle indicates up and down regulation of luciferase expression, respectively. Out of the 64,755 siRNA's tested 1,681 significantly enhanced luciferase expressions (MAD-based z-score > 3, or 40% to 178% higher than negative control). From these 1,681 siRNAs, 56 genes with at least 2 siRNAs scoring > 3 MAD were selected and subjected to follow up evaluation with additional siRNAs.11,207 (17.3%) of the siRNAs tested, listed in Table S3, improved per cell luciferase expression by more than 20% (Fig. 1C quadrant I&II), while only 254(0.4%) of the siRNAs tested, listed in Table S2, achieved more than 20% enhancement in viable cell density (Fig. 1C quadrant I&IV). The 168 siRNAs associated with the 56 selected genes are indicated by red or orange circles, in which red was used as the colour for siRNAs with > 3 MAD score,

2. Identification of pathways affecting viable cell density and recombinant protein productivity

To identify pathways that affect the reporter protein production, functional ontology analyses were carried out using the 119 siRNAs (Table 3) against the 56 genes that significantly improved the specific luciferase yield, using the PANTHER (http://www.pantherdb.org/) (Mi et al., 2013) and AmiGO 2 GO browser (Carbon et al., 2009). The heat map (Figure 2) shows that all the siRNAs enhanced per cell luciferase yield (pink to red spectrum), but the majority negatively affected the cell viability (blue shades) which is undesirable in recombinant protein production. The enhancer siRNAs were found to be enriched in the following specific pathways: mRNA processing/spliceosome, transcription, metabolic process, cation transport and protein folding.

3. Selection of ten genes whose silencing leads to enhanced luciferase expression

For selecting gene candidates for further work, three additional siRNAs were tested for each of the 56 target genes identified from the primary screen. From the combined data of the primary and the validation screen of the 56 genes, ten genes were selected, based on the criteria that at least 3 out of the 6 siRNAs tested displayed a MAD-based z-scores higher than 3.0 (Table 1). The viable cell number was also taken into consideration to remove candidates with significant toxicity. The median value of the overall luciferase yield for each selected gene calculated from the 6 siRNAs was improved by 24% to 72% compared with negative control, and the median of MAD-based z-scores ranged from 2.13 to 4.55.

Four out of the ten target genes, *INTS1, INTS2, HNRNPC*, and *PRPF19*, are involved in mRNA splicing process; they encode important proteins for spliceosome formation, such as integrator complex, heterogeneous nuclear ribonucleoprotein and pre-mRNA processing factor 19. The remainder of the identified genes encodes proteins involved in a wide span of biological functions, including cell growth and division, signal transduction, apoptosis, regulation of cellular polyamine concentration and protein translation and folding.

4. Effects of silencing the ten target genes on secreted and membrane protein production

To examine the silencing effect of the 10 selected genes on the expression of other recombinant proteins from HEK293 cells, three additional cell lines were tested: 1) HEK-GPC3-hFc cell line, which constitutively secretes glypican −3 hFc-fusion protein (GPC3-hFc) (Feng et al., 2013) as a representative of antibody secreting cell lines, 2) T-REx-293-

NTSR1-GFP cell line constructed previously for the production of functional neurotensin receptor type I (NTSR1)(Xiao et al., 2015) and 3) T-REx-293-SERT-GFP cell line (Abdul-Hussein et al., 2013), an inducible cell line for high level expression of serotonin transporter (SERT), a “hard-to-express” 12 transmembrane domain protein. Both NTRS1 and SERT were fused with GFP at the C-terminus, allowing proximal protein quantification by flow cytometry. As shown in Figure 3, the siRNAs against the ten selected genes exhibited varying effects on the expression of the secreted and the membrane proteins. The silencing of *INTS1, HNRHPC, OAZ1* and *PPP2R1A* consistently improved the expression of all reporter proteins tested. However, the silencing of *INTS1* and *HNRNPC* led to a significantly reduced viable cell number, an indication that these genes may be essential for cell survival or cell growth. Silencing of the *OAZ1* and *PPP2R1A* genes showed minimal negative effects on the viable cell number.

5. Effect of silencing *OAZ1* on luciferase expression

Among the selected genes, the antizyme 1 (*OAZ1*) was chosen for follow-up studies since its silencing consistently improved cytosolic, secreted and membrane protein expression and caused minimal growth disadvantage in the four cell lines tested (Figure 3). Five of the six OAZ1siRNAs tested (Table 2) enhanced luciferase production (luciferase activity (%)) by 28–74%, and OAZ1 siRNA5 was chosen for the rest of the study. Unlike OAZ1 siRNAs, the siRNAs against antizyme isoforms OAZ2 (a minor isoform) and OAZ3 (a testis specific form) caused no significant enhancement of luciferase production (Table 2).

As cells transfected with siOAZ1 showed significantly higher luciferase production for an extended period of time (Figure 4A), the efficacies of silencing antizyme 1 was evaluated with qRT-PCR (Figure 4B). The expression of OAZ1 mRNA in the 24–72 hour period following the transfection of siRNA, was less than 3% compared with negative control siRNA-transfected cells, confirming the silencing by the siRNA. Throughout the 96 hour period luciferasem RNA levels did not increase and remained somewhat lower than those of negative control cells (Figure 4C), an indication that the enhanced luciferase production is the result of an increased translation.

6. Effect of silencing *OAZ1* on ornithine decarboxylase (ODC) and cellular polyamines

OAZ1 is a negative regulator of the ODC, a rate-limiting enzyme in the polyamine biosynthesis (Coffino, 2001; Kahana, 2009; Pegg, 2006). OAZ1 inactivates ODC by forming heterodimers with the ODC monomer and by directing the protein to degradation by the 26S proteasome (Miyazaki et al., 1992; Murakami et al., 1992). OAZ1 itself is regulated by antizyme inhibitor (AZIN), an ODC-like protein that increase the ODC concentration as a result of reducing OAZ (Scheme 1). As seen in Figure 5A, the silencing of OAZ1 with siRNA increased significantly the ODC level from 24 to 96 hours, as was expected from the known inhibitory effect of OAZ1 on ODC. But at the same time little or no change in the ODC level was observed in the un-transfected and in the negative controlled transfected cells. The elevated ODC is obviously not the result of enhanced ODC transcription, since qRT-PCR analysis shown consistent reduction of ODC mRNA levels after *OAZ1* silencing (Figure 5B). As seen in Figure 5C, silencing *OAZ1* caused changes in cellular polyamine levels; the putrescine concentration was 10 fold higher compared with the negative control

cells. Spermidine concentration was increased to a lesser extent, whereas spermine was either unchanged or reduced.

7. Effects of exogenous polyamines on luciferase protein expression

Increased cellular polyamines in *OAZ1*-silenced cells are most likely responsible for the enhanced cellular production of the reporter proteins. To further verify this, the impacts of exogenously added polyamines on luciferase expression level and viable cell number were determined. As can be seen in Figure 6A, up to 40% increase of luciferase expression was observed when putrescine was added to medium at 100 μM and 10% enhanced growth was observed with putrescine addition at 50 μM. Higher concentrations did not lead to further enhancement of luciferase production. The spermidine effect is seen in Figure 6B; 36% increase in luciferase expression was observed at 20 μM, and 24% increase in cell growth was achieved at 10 μM. In case of spermine addition, only 16% increase in luciferase expression was observed at 10 μM and higher concentrations caused reduction in both luciferase expression and viable cell(Figure 6C). The inhibitory effects of spermidine (>100 μM) and spermine (>20 μM) are probably due to generation of the toxic oxidation products by ruminant serum oxidases present in the culture medium (Pegg, 2013).

Discussion

Cultured mammalian cells are the dominant vehicle for production of recombinant proteins for bio-therapeutics and structural studies. As a result, continuous effort has been directed toward improving cellular production capabilities. Previous work (Xiao et al., 2014) demonstrated the ability to improve recombinant protein expression based primarily on knowledge of specific genes and pathways, yet there is a need for discovering novel genes and pathways for further improvement of production. Genome-wide screening using SiRNA has emerged as a powerful tool for probing gene functions and for target discovery in various diseases (Bard et al., 2006; Brognard and Hunter, 2011; Cherry, 2008; Ni and Lee, 2010; Orvedahl et al., 2011). However, it has rarely been used to identify targets for enhanced recombinant protein production (Bard et al., 2006; Simpson et al., 2012).The purpose of the present study was is to discover new candidates suitable for improving recombinant protein production from HEK 293 cells, by performing high throughput RNA interference screen.

An HEK293 cell line expressing the luciferase reporter was subjected to interference with 64,755 siRNAs targeting 21,585 human genes. 1,681 siRNAs (2.6% of the library) improved the luciferase expression with an MAD-based z-score >3. To eliminate the introduction of ‘false positives’ due to off-target effects, gene hits were considered ‘true positives’ only if more than two single siRNAs targeting the gene passed the MAD-based z-score >3. As a result, fifty six genes were selected and validated with 3 additional siRNAs for each gene. From the data generated by the six siRNAs for each of the 56 genes, ten genes were selected for further analysis. These genes showed an increase in luciferase yield of 3 MAD-based z-scores by 3 or more siRNAs, corresponding to a 40% increase in luciferase activity.

The effects of the siRNAs targeting the ten identified genes on recombinant protein expression from the HEK cells were assessed further by measuring the expression of three

additional recombinant proteins: a secreted protein (GPC3-hFc) and two “hard-to-express” membrane proteins (neurotensin receptor type I and serotonin transporter). Silencing of the *INTS1, HNRHPC, OAZ1*, and *PPP2R1A* genes consistently improved production of all the tested proteins. Of these four genes, silencing *INTS1* or *HNRHPC* affected cell viability of the other two genes that only slightly affected the cell, *OAZ1* was chosen for follow-up studies.

The identification of *OAZ1* as a gene whose silencing can enhance recombinant protein production is an indication that this gene normally suppresses protein synthesis. This is compatible with the known function of theOAZ1 as a negative regulator of polyamine homeostasis, cell proliferation and transformation (Bercovich et al., 2011; Coffino, 2001; Kahana, 2009; Pegg, 2006). OAZ1 is a negative regulator of ODC, a rate-limiting enzyme in polyamine biosynthesis. OAZ1 itself is known to be regulated by AZIN, an ODC-like protein that increases the ODC concentration as a result of reducing OAZ1 concentration (Scheme 1). Silencing of *OAZ1* was also associated with increased cellular levels of putrescine and spermidine, and addition of external putercine and spermidine caused increased protein expression in the control cells. The observation that increasing the concentration of cellular putrescine and spermidine increases the biosynthesis of reporter proteins without increasing their transcription provides new insights into the primary function of polyamines in the regulation of translation. Consistent with this observation is published information (Mandal et al., 2013) that depleting cellular spermidine and spermine by over-expressing spermidine/spermine N^1 -acetyltransferase 1(SSAT1) led to suppression of protein biosynthesis without inhibiting DNA and RNA biosynthesis. We believe that this report is the first to identify polyamine pathways as promising targets for improved recombinant protein production.

Supplementary Material

Refer to Web version on PubMed Central for supplementary material.

Acknowledgments

The authors thank Dr E. C. Wolff (NIDCR, NIH) and Mrs. D Livnat for critical reading of the manuscript and editorial assistance, Dr R Grisshammer (NINDS/NIH) for providing NTSR1 construct, Dr C.G. Tate (MRC Cambridge, UK) for the T-Rex-SERT-GFP cell line, Dr M Ho (NCI/NIH) for HEK-GPC3-hFc cell line.

Funding

The research was supported by the Intramural Research Program of National Institute of Diabetes and Digestive and Kidney Diseases (NIDDK/NIH), National Center for Advancing Translational Sciences (NCATS/NIH) and the National Institute of Dental and Craniofacial Research (NIDCR/NIH)

References

Aagaard L, Rossi JJ. RNAi therapeutics: principles, prospects and challenges. Adv. Drug Deliv. Rev. 2007; 59(2–3):75–86. [PubMed: 17449137]

Abdul-Hussein S, Andrell J, Tate CG. Thermostabilisation of the serotonin transporter in a cocaine-bound conformation. J Mol Biol. 2013; 425(12):2198–2207. [PubMed: 23706649]

Bard F, Casano L, Mallabiabarrena A, Wallace E, Saito K, Kitayama H, Guizzunti G, Hu Y, Wendler F, DasGupta R, Perrimon N, Malhotra V. Functional genomics reveals genes involved in protein secretion and Golgi organization. Nature. 2006; 439(7076):604–607. [PubMed: 16452979]

Bercovich Z, Snapir Z, Keren-Paz A, Kahana C. Antizyme affects cell proliferation and viability solely through regulating cellular polyamines. J Biol Chem. 2011; 286(39):33778–33783. [PubMed: 21832059]

Brognard J, Hunter T. Protein kinase signaling networks in cancer. Curr Opin Genet Dev. 2011; 21(1): 4–11. [PubMed: 21123047]

Carbon S, Ireland A, Mungall CJ, Shu SQ, Marshall B, Lewis S. AmiGO: online access to ontology and annotation data. Bioinformatics. 2009; 25(2):288–289. [PubMed: 19033274]

Carr, D. hexbin:Hexagonal Binning Routines R package version 1.27.1. 2015. http://CRAN.R-project.org/package=hexbin

Cherry S. Genomic RNAi screening in *Drosophila* S2 cells: what have we learned about host-pathogen interactions? Curr Opin Microbiol. 2008; 11(3):262–270. [PubMed: 18539520]

Chung N, Zhang XD, Kreamer A, Locco L, Kuan PF, Bartz S, Linsley PS, Ferrer M, Strulovici B. Median absolute deviation to improve hit selection for genome-scale RNAi screens. J Biomol Screen. 2008; 13(2):149–158. [PubMed: 18216396]

Coffino P. Regulation of cellular polyamines by antizyme. Mol Cell Biol. 2001; 2(3):188–194.

Conrad C, Gerlich DW. Automated microscopy for high-content RNAi screening. J Cell Biol. 2010; 188(4):453–461. [PubMed: 20176920]

Feng M, Gao W, Wang R, Chen W, Man YG, Figg WD, Wang XW, Dimitrov DS, Ho M. Therapeutically targeting glypican-3 via a conformation-specific single-domain antibody in hepatocellular carcinoma. Proc Natl Acad Sci USA. 2013; 110(12):E1083–E1091. [PubMed: 23471984]

Hamilton AJ, Baulcombe DC. A species of small antisense RNA in posttranscriptional gene silencing in plants. Science. 1999; 286(5441):950–952. [PubMed: 10542148]

Huang, da W., Sherman, BT., Lempicki, RA. Systematic and integrative analysis of large gene lists using DAVID bioinformatics resources. Nat Protoc. 2009; 4(1):44–57. [PubMed: 19131956]

Jinek M, Doudna JA. A three-dimensional view of the molecular machinery of RNA interference. Nature. 2009; 457(7228):405–412. [PubMed: 19158786]

Kahana C. Antizyme and antizyme inhibitor, a regulatory tango. Cell Mol Life Sci. 2009; 66(15): 2479–2488. [PubMed: 19399584]

Livak KJ, Schmittgen TD. Analysis of relative gene expression data using real-time quantitative PCR and the 2(−Delta Delta C(T)) Method. Methods. 2001; 25(4):402–408. [PubMed: 11846609]

Mandal S, Mandal A, Johansson HE, Orjalo AV, Park MH. Depletion of cellular polyamines, spermidine and spermine, causes a total arrest in translation and growth in mammalian cells. Proc Natl Acad Sci USA. 2013; 110(6):2169–2174. [PubMed: 23345430]

Mi H, Muruganujan A, Casagrande JT, Thomas PD. Large-scale gene function analysis with the PANTHER classification system. Nat Protoc. 2013; 8(8):1551–1566. [PubMed: 23868073]

Miyazaki Y, Matsufuji S, Hayashi S. Cloning and characterization of a rat gene encoding ornithine decarboxylase antizyme. Gene. 1992; 113(2):191–197. [PubMed: 1572540]

Murakami Y, Matsufuji S, Kameji T, Hayashi S, Igarashi K, Tamura T, Tanaka K, Ichihara A. Ornithine decarboxylase is degraded by the 26S proteasome without ubiquitination. Nature. 1992; 360(6404):597–599. [PubMed: 1334232]

Napoli C, Lemieux C, Jorgensen R. Introduction of a chimeric chalcone synthase gene into petunia results in reversible co-suppression of homologous genes *in trans* . Plant Cell. 1990; 2(4):279–289. [PubMed: 12354959]

Ni Z, Lee SS. RNAi screens to identify components of gene networks that modulate aging in *Caenorhabditis elegans* . Brief Funct Genomics. 2010; 9(1):53–64. [PubMed: 20053814]

Orvedahl A, Sumpter R Jr, Xiao G, Ng A, Zou Z, Tang Y, Narimatsu M, Gilpin C, Sun Q, Roth M, Forst CV, Wrana JL, Zhang YE, Luby-Phelps K, Xavier RJ, Xie Y, Levine B. Image-based genome-wide siRNA screen identifies selective autophagy factors. Nature. 2011; 480(7375):113–117. [PubMed: 22020285]

Pegg AE. Regulation of ornithine decarboxylase. J Biol Chem. 2006; 281(21):14529–14532. [PubMed: 16459331]

Pegg AE. Toxicity of polyamines and their metabolic products. Chem Res Toxicol. 2013; 26(12): 1782–1800. [PubMed: 24224555]

R Core Team. A language and environment for statistical computing. 2015. www.R-project.org

Seyhan AA, Rya TE. RNAi screening for the discovery of novel modulators of human disease. Curr Pharm Biotechnol. 2010; 11(7):735–756. [PubMed: 20420566]

Simpson JC, Joggerst B, Laketa V, Verissimo F, Cetin C, Erfle H, Bexiga MG, Singan VR, Hériché JK, Neumann B, Mateos A, Blake J, Bechtel S, Benes V, Wiemann S, Ellenberg J, Pepperkok R. Genome-wide RNAi screening identifies human proteins with a regulatory function in the early secretory pathway. Nat Cell Biol. 2012; 14(7):764–774. [PubMed: 22660414]

van der Krol AR, Mur LA, Beld M, Mol JN, Stuitje AR. Flavonoid genes in petunia: addition of a limited number of gene copies may lead to a suppression of gene expression. Plant Cell. 1990; 2(4):291–299. [PubMed: 2152117]

Wickham, H. ggplot2:elegant graphics for data analysis. New York: Springer; 2009. p. 213p

Xiao S, Shiloach J, Betenbaugh MJ. Engineering cells to improve protein expression. Curr Opin Struct Biol. 2014; 26:32–38. [PubMed: 24704806]

Xiao S, Chen YC, Betenbaugh MJ, Martin SE, Shiloach J. MiRNA mimic screen for improved expression of functional neurotensin receptor from HEK293 cells. Biotechnol Bioeng. 2015; 112(8):1632–1643. [PubMed: 25676429]

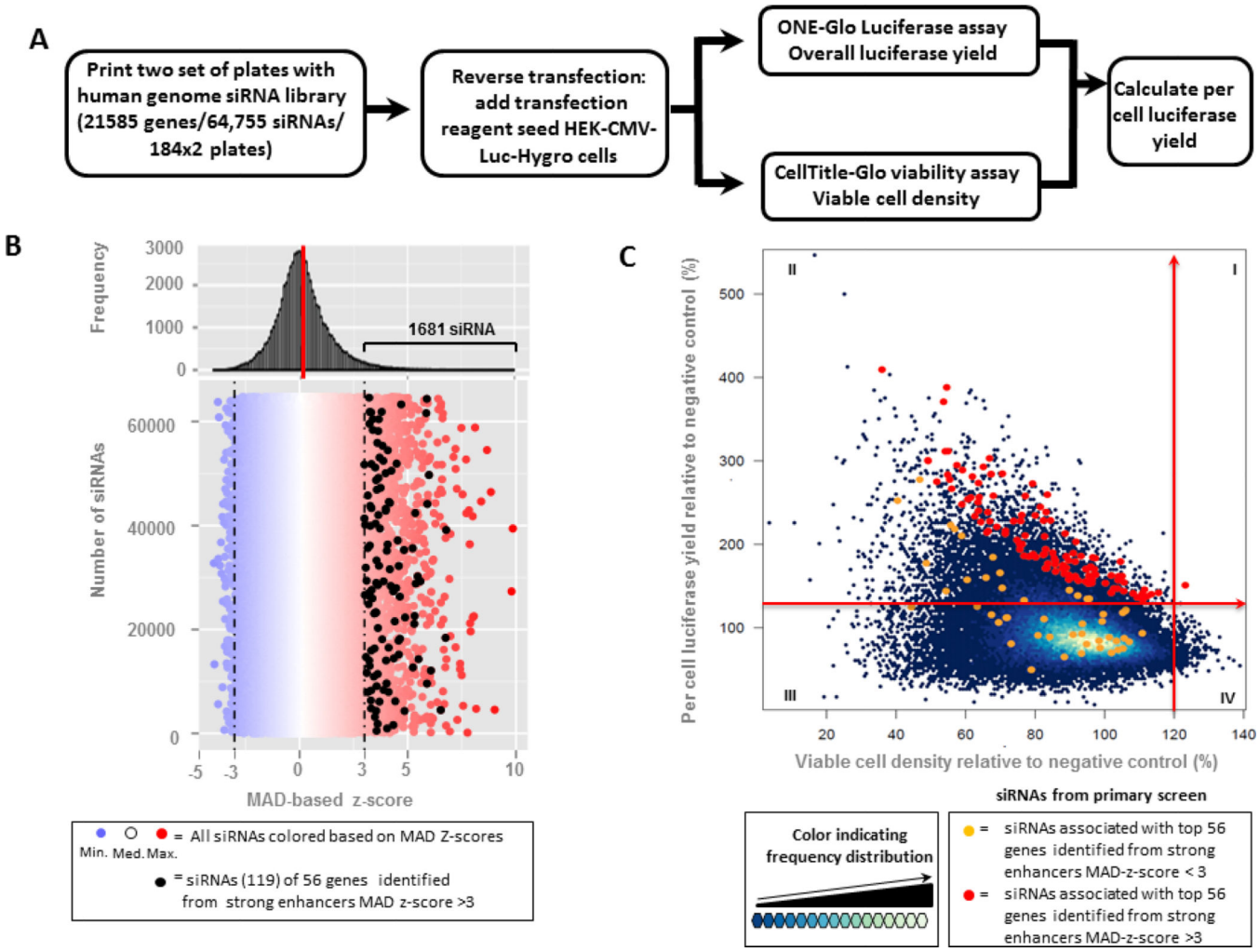

Fig. 1. Genome-wide human siRNA library screen with HEK-CMV-luc2-Hygro cell line

(A) Workflow of the primary screen; (B) Distribution of siRNA effect on improved overall luciferase expression, The 119 siRNAs corresponding to 56 identified genes with strong enhancer MAD z-score (>3) are indicated as black circles. (C)Relative per cell luciferase yield as a function of the relative cell viability for each sRNA tested. The 20% increase cut-offs are highlighted and divide the entire population into quadrants (I, II, III and IV). siRNAs associated with top 56 genes with a MAD-z score>3 are indicated as red circles and those with MAD-z-score < 3 as orange circles.

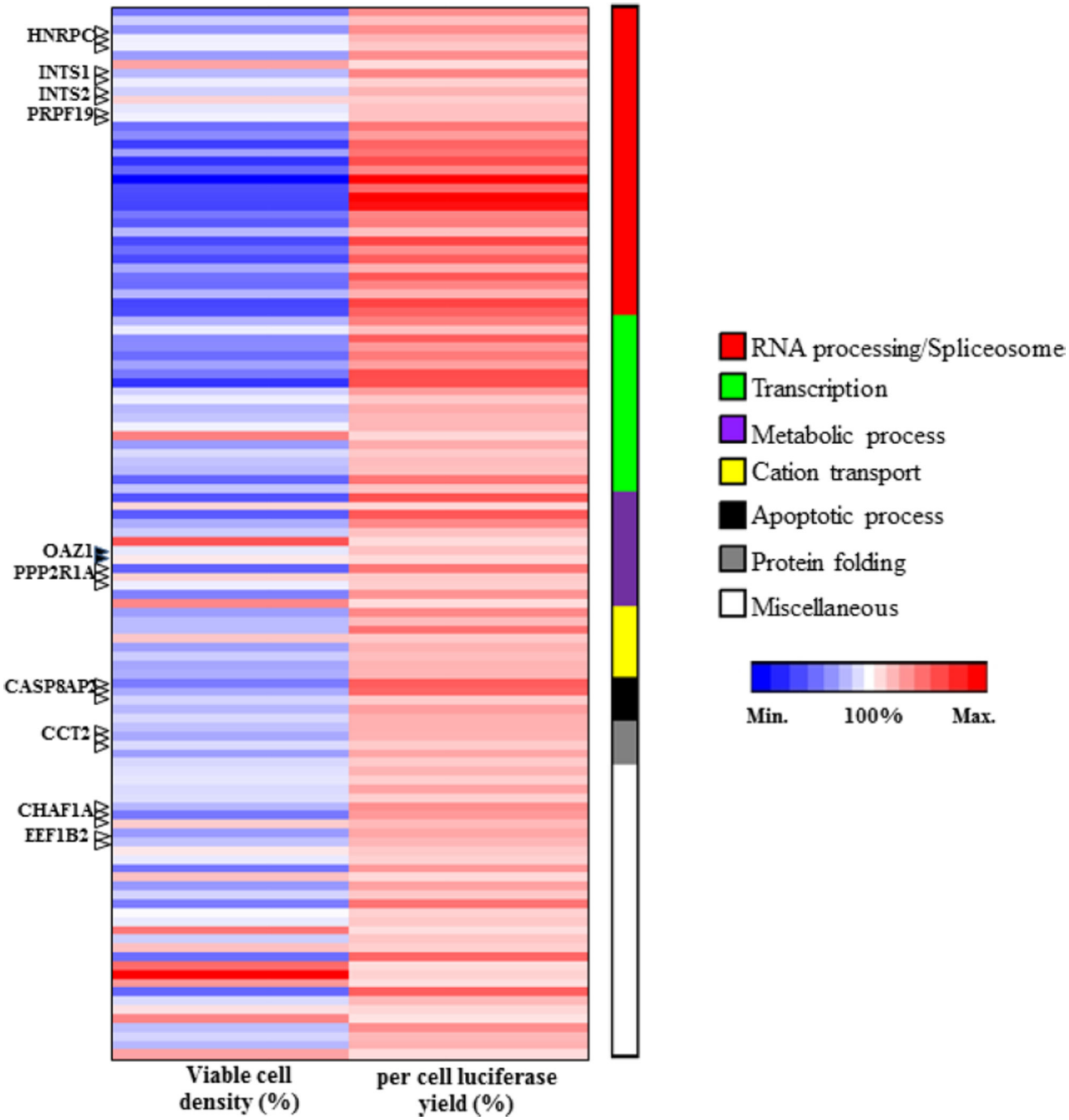

Fig. 2. Functional categorization of strong enhancer siRNA-associated genes

Heat map was generated based on percent viable cell density and per cell luciferase yield for each of the 119 siRNAs that significantly enhanced luciferase production. The values are indicated by range of red (maximum) and blue (minimum) intensities. The functional categories are indicated by bars of different colours and the numbers of siRNAs in each group indicated by the bar lengths.

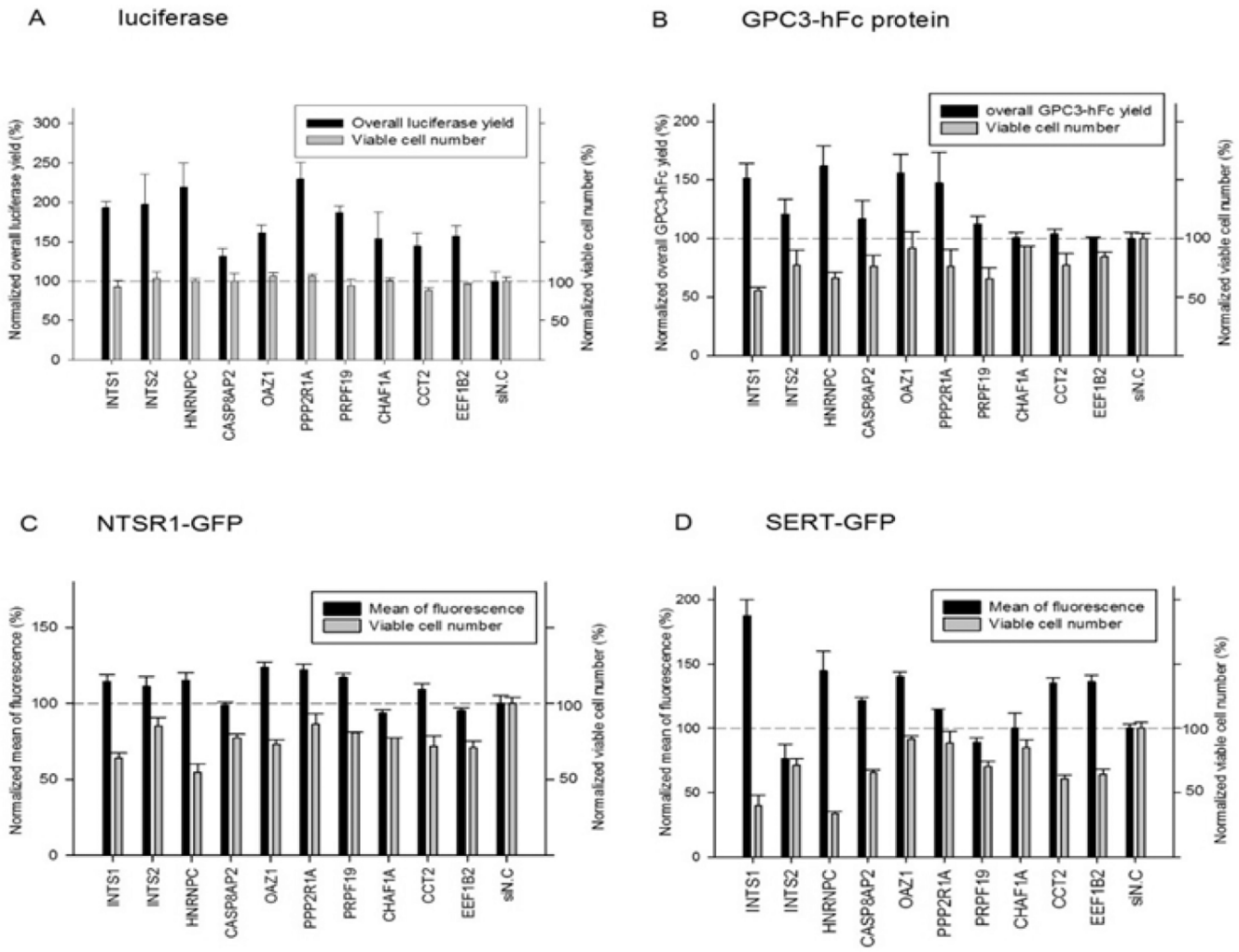

Fig. 3. Effects of the 10 selected enhancer siRNAs on four HEK cell lines expressing different recombinant proteins

(A) Luciferase, (B) GPC3-hFc, (C) NTSR1-GFP, (D) SERT-GFP; Protein expression and cell viability were normalized against cells transfected with the negative control siRNA (si N.C.). The experiment was performed twice with different passages of cells. For each biological sample, the measurement was done in duplicates. Error bars indicate standard error of the mean (SEM).

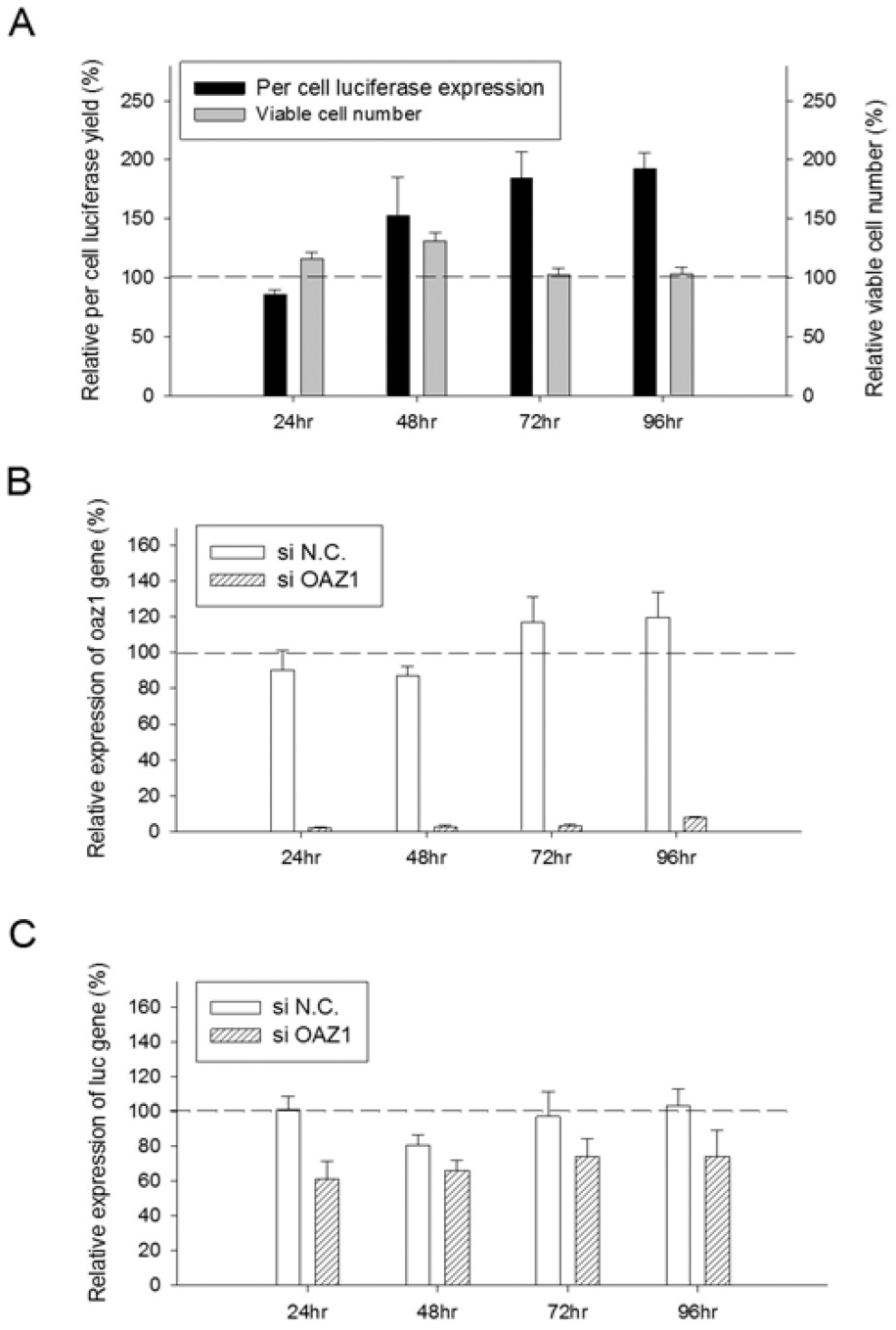

Fig. 4. Effects of OAZ1 siRNA transfection on cell viability, luciferase yield, mRNA levels of OAZ1 and mRNA levels of luciferase

(A) Cell viability and luciferase protein expression; (B) Relative expression of OAZ1-mRNA; (C) Relative expression of luciferase mRNA. The relative levels of luciferase yield and cell viability in the OAZ1 siRNA-transfected cells were compared to those of cells transfected with negative control siRNA (siN.C.) Transfection was done with two different passages of cells and each biological sample was measured in triplicates. Error bars represent SEM.

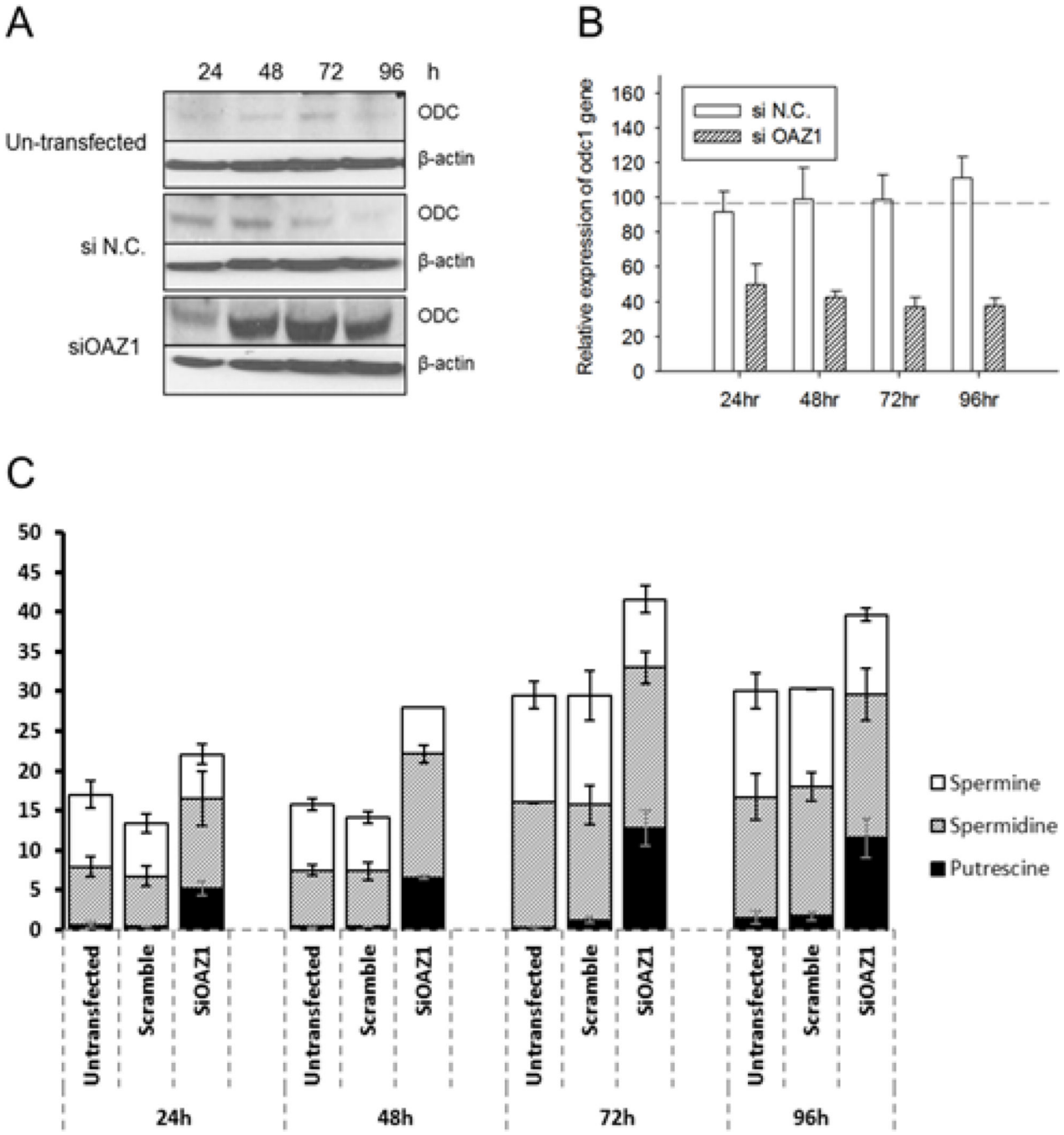

Fig. 5. Effects of silencing *OAZ1* on the ODC protein levels, on ODC mRNA and on cellular polyamines

(A) Western blot of ODC, (B) ODC mRNA level, (C) Cellular polyamines concentration. Polyamine concentrations were normalized against total protein and presented as nmol/mg total protein. Transfection was done with two different passages of cells and each biological sample was measured in triplicates. Error bars represent SEM. si N.C. indicates control scramble siRNA.

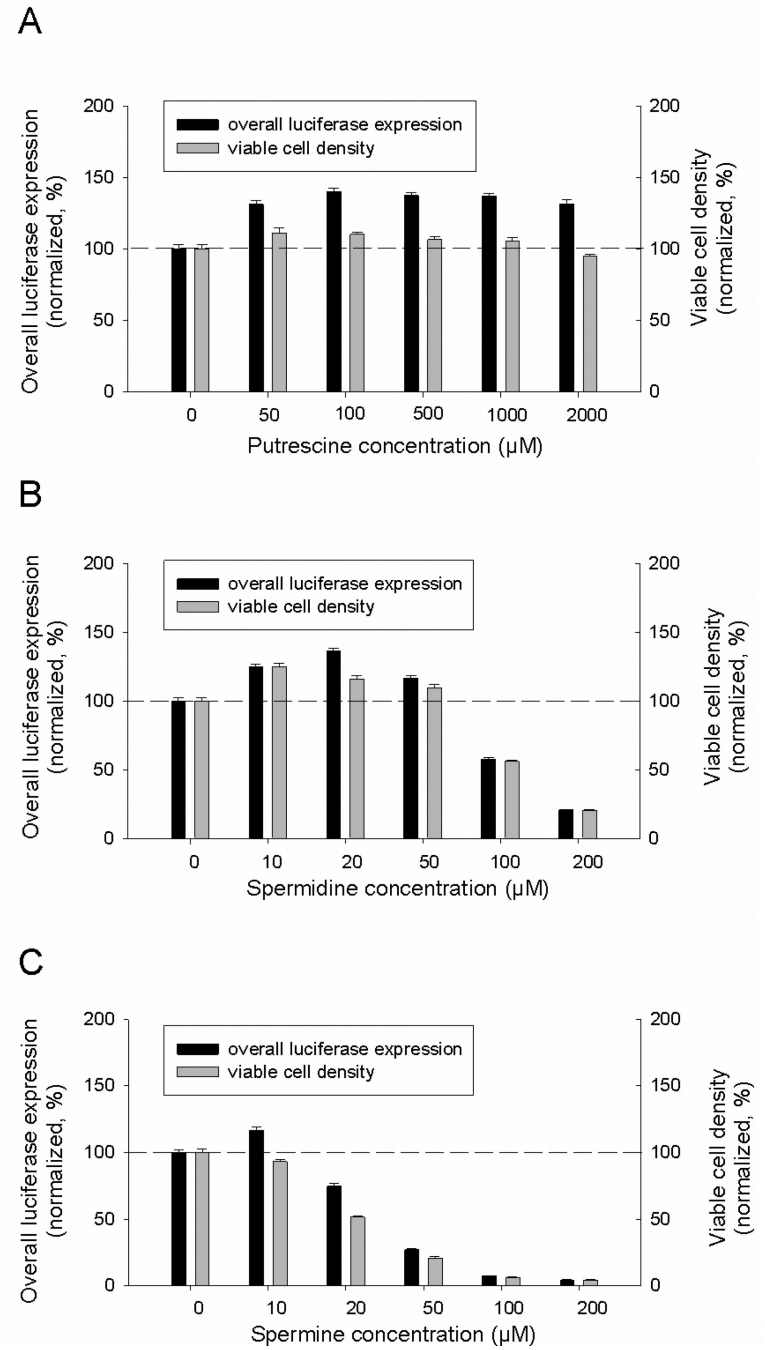

Fig. 6. Effect of exogenous polyamines on luciferase expression and cell growth

Two different passages of cells were treated with the indicated concentrations of polyamines and each biological sample was measured in triplicates. Error bars represent SEM.

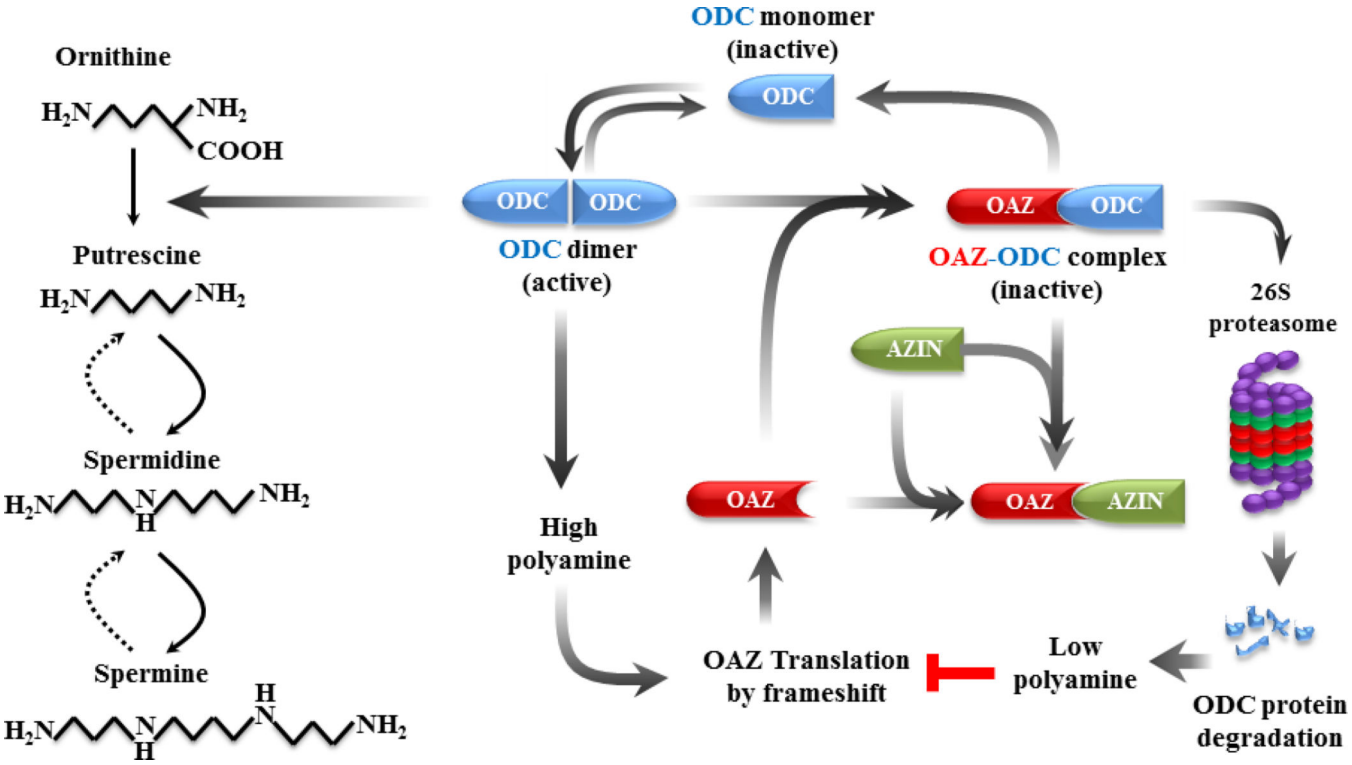

Scheme 1. Schematic diagram of polyamine pathway and regulation of ornithine decarboxylase (ODC) by antizyme (OAZ) and antizyme inhibitor (AZIN)

Simplified pathway of polyamine synthesis from ornithine is indicated by solid arrows and polyamine catabolism by broken arrows. ODC is regulated by OAZ whose translation is turned on by +1 ribosomal frame shifting at a high concentration of polyamines. OAZ is in turn regulated by AZIN, which is an ODC-like protein, but devoid of the enzyme activity.

Table 1

Confirmed top 10 genes with 3 or more siRNAs yielding > 50% increase in luciferase activity. A 50% increase is biologically relevant and also corresponds to high statistical significance (>3 MAD-based z-scores).

Gene	Description	Overall luciferase yield (%)*,†	MAD-based z-score*	Viable cell density (%)*,†	MAD-based z-score*	Function
INTS1	Integrator Complex Subunit 1	172	4.55	96	0.46	3'- end processing of small nuclear RNAs U1 and U2
INTS2	Integrator Complex Subunit 2	165	4.17	89	−0.11	3'- end processing of small nuclear RNAs U1 and U2
HNRNPC	Heterogeneous Nuclear Ribonucleoprotein	163	4.10	97	0.48	Influencing pre-mRNA processing and other aspects of mRNA metabolism and transport
CASP8AP2	Caspase 8 Associated Protein 2	156	3.70	79	−0.86	Activation and regulation of CASP8 in FAS-mediated apoptosis
OAZ1	Ornithine Decarboxylase Antizyme	153	3.57	115	0.36	Inhibiting ornithine decarboxylase and inactivating the polyamine uptake transporter
PPP2R1A	Protein Phosphatase 2, Regulatory Subunit A, Alpha	153	3.56	96	0.46	Serving as a scaffold for Protein Phosphatase 2 assembly, essential for signal transduction pathways
PRPF19	Pre-mRNA Processing Factor 19	147	3.27	96	0.41	Spliceosome assembly and activating pre-mRNA splicing
CHAF1A	Chromatin Assembly Factor 1, Subunit A	138	2.80	82	−0.62	mediating chromatin assembly in DNA replication and DNA repair
CCT2	Chaperonin Containing TCP1, Subunit 2 (Beta)	126	2.23	85	−0.41	Chaperonin-mediated protein folding of actin, tubulin and other proteins
EEF1B2	Eukaryotic Translation Elongation Factor 1 Beta 2	124	2.13	85	−0.38	exchanging GDP bound to EF-1-α to GTP during the transfer of aminoacylated tRNAs to the ribosome

*All values are medians of result from 6 siRNAs (3 siRNAs in primary screen and 3 siRNAs in validation screen) targeting a top gene.

†Values are normalized to negative control siN.C. transfected cells (set as 100%).

Table 2

The list of siRNAs targeting the polyamine pathway genes, OAZ1, OAZ2, OAZ3, ODC and AZIN1 and their effects on luciferase activity, cell viability and per cell luciferase yield. The data are from the primary siRNA screen, except for the last three additional siRNAs against OAZ1

Gene Symbol	siRNA sequence	Luciferase activity (%)	Viable cell number (%)	Per cell luciferase yield (%)
OAZ1	GCCUUGCUCCGAACCUUCAtt	161.1	94.8	169.9
	GAUUAUCCUUGUACUUUGAtt	144.5	101.9	141.8
	GGCUGAAUGUAACAGAGGAtt	127.6	94.9	134.5
	CCGUAGACUCGCUCAUCUCtt	174.4	85.4	204.2
	GCUAACUUAUUCUACUCCGtt	171.1	110.6	154.7
	GGGAAUAGUCAGAGGGAUCtt	92.8	102.7	90.4
OAZ2	ACAUCGUCCACUUCCAGUAtt	97.4	96.3	101.1
	GGACCUCCCUGUGAAUGAUtt	95.4	86.0	110.9
	CAGAUGGAUUAUUAGCUGAtt	94.9	105.4	90.0
OAZ3	CCGGGAAAGUUUGACUGCAtt	101.5	75.8	133.9
	CCACGACCAGCUUAAAGAAtt	90.5	95.76	94.5
	GACUUUCACUUCCGCCUUAtt	74.3	87.7	84.7
ODC1	GAUGACUUUUGAUAGUGAAtt	18.0	56.1	32.1
	GCAUGUAUCUGCUUGAUAUtt	20.0	50.7	39.4
	GCUUGCAGUUAAUAUCAUUtt	28.4	60.8	46.7
AZIN1	CACUCGCAGUUAAUAUCAUtt	25.2	64.6	39.0
	CGAUGAACAUGUUAGACAUtt	30.4	72.1	42.2
	GCCCUCUGUUGGAUAUCUAtt	45.6	72.1	63.2

Table 3

List of the 119 SiRNA targeting the selected 56 genes

No.	Symbol	Viable cell density (%)	per cell luciferase yield (%)	Gene_ID	siRNA sequence	Biological process
1	APOBEC3H	66.938	227.583	164668	AGAGGCUACUUUGAAAACAtt	RNA processing/Spliceosome
2	APOBEC3H	88.955	171.805	164668	CAAGUCACCUGUUACCUCAtt	RNA processing/Spliceosome
3	HNRNPC	73.809	227.741	3183	ACACUCUUGUGGUCAAGAAtt	RNA processing/Spliceosome
4	HNRNPC	96.599	184.201	3183	GAUGAAGAAUGAUAAGUCAtt	RNA processing/Spliceosome
5	HNRNPC	97.392	163.496	3183	CAACGGGACUAUUAUGAUAtt	RNA processing/Spliceosome
6	HNRPDL	75.879	227.884	9987	CCCGGAUACUUCUGAAGAAtt	RNA processing/Spliceosome
7	HNRPDL	108.214	140.868	9987	GAACGAGUACAGCAAUAUAtt	RNA processing/Spliceosome
8	INTS1	83.129	238.606	26173	GUUCAUCCAUAAGUACAUUtt	RNA processing/Spliceosome
9	INTS1	96.256	153.438	26173	AGAUCUUUGUCAAGGUGUAtt	RNA processing/Spliceosome
10	INTS2	88.908	185.522	57508	GACAUUGGAUCAUACUAAAtt	RNA processing/Spliceosome
11	INTS2	103.888	156.977	57508	GGCGAAUGCUCCUGACUAAtt	RNA processing/Spliceosome
12	PRPF19	94.579	170.349	27339	GCGCAAGCUUAAGAACUUUtt	RNA processing/Spliceosome
13	PRPF19	97.007	170.088	27339	GCUCAUCGACAUCAAAGUUtt	RNA processing/Spliceosome
14	RBM22	63.879	256.443	55696	CCAUAUAUCCGAAUGACCAtt	RNA processing/Spliceosome
15	RBM22	71.395	212.652	55696	CGGAAUCAAUGAUCCUGUAtt	RNA processing/Spliceosome
16	SART1	51.696	275.068	9092	GCAUCGAGGAGACUAACAAtt	RNA processing/Spliceosome
17	SART1	77.169	257.929	9092	CAAUGAUUCUUACCCUCAAtt	RNA processing/Spliceosome

No.	Symbol	Viable cell density (%)	per cell luciferase yield (%)	Gene_ID	siRNA sequence	Biological process
18	SF3B3	49.133	300.611	23450	CAACCUUAUUAUCAUUGAAtt	RNA processing/Spliceosome
19	SF3B3	62.659	233.649	23450	GUUUCAUCUGGGUUCGCUAtt	RNA processing/Spliceosome
20	SF3B4	35.915	409.361	10262	GCAUCAGCUCACAACAAAAtt	RNA processing/Spliceosome
21	SF3B4	55.962	266.627	10262	GUCCUAUCACCGUAUCUUAtt	RNA processing/Spliceosome
22	SNRPB	54.559	388.072	6628	AGAUACUGGUAUUGCUCGAtt	RNA processing/Spliceosome
23	SNRPB	53.645	370.824	6628	UGGUCUCAAUGACAGUAGAtt	RNA processing/Spliceosome
24	SNRPB	66.394	238.463	6628	GGCUGUACAUAGUCCUUUUtt	RNA processing/Spliceosome
25	SNRPD2	58.901	247.842	6633	UGUGGACUGAGGUACCCAAtt	RNA processing/Spliceosome
26	SNRPD2	82.950	171.198	6633	CUGCCGCAACAAUAAGAAAtt	RNA processing/Spliceosome
27	SNRPE	54.945	311.516	6635	GGAUCAUGCUAAAAGGAGAtt	RNA processing/Spliceosome
28	SNRPE	64.385	226.659	6635	CAUUGGUUUUGAUGAGUAUtt	RNA processing/Spliceosome
29	SNRPF	54.854	283.281	6636	AGGGCUAUCUGGUAUCUGUtt	RNA processing/Spliceosome
30	SNRPF	79.386	188.094	6636	GGUGUAAUAAUGUCCUUUAtt	RNA processing/Spliceosome
31	U2AF1	65.083	292.710	7307	GAAUAACCGUUGGUUUAAUtt	RNA processing/Spliceosome
32	U2AF1	63.672	240.287	7307	GGAACACUAUGAUGAGUUUtt	RNA processing/Spliceosome
33	U2AF1	82.333	187.362	7307	GGUGCUCUCGGUUGCACAAtt	RNA processing/Spliceosome
34	U2AF2	54.133	311.348	11338	CCAACUACCUGAACGAUGAtt	RNA processing/Spliceosome
35	U2AF2	55.405	277.511	11338	CAGCAAACCUUUGACCAGAtt	RNA processing/Spliceosome
36	CNOT1	81.492	244.722	23019	GCUAUUUCCAGCGAAUAUAtt	Transcription
37	CNOT1	96.002	173.284	23019	GGAGGAAUCUCGAAUGCGAtt	Transcription

No.	Symbol	Viable cell density (%)	per cell luciferase yield (%)	Gene_ID	siRNA sequence	Biological process
38	KAT5	70.586	284.565	10524	GGAGAAAGAAUCAACGGAAtt	Transcription
39	KAT5	71.473	216.209	10524	GGACGGAAGCGAAAAUCGAtt	Transcription
40	L3MBTL4	63.577	250.367	91133	GAACUUCAAUGGAAAACAUtt	Transcription
41	L3MBTL4	77.107	210.336	91133	GAUCGUUUGAGAGAACAAAtt	Transcription
42	MZF1	66.872	302.994	7593	CAGGUAGUGUAAGCCCUCAtt	Transcription
43	MZF1	49.189	299.886	7593	AGGUUACAGAGGACUCAGAtt	Transcription
44	NKX3-2	88.616	212.905	579	GAACCGUCGCUACAAGACAtt	Transcription
45	NKX3-2	96.869	162.999	579	CCCUCCUACUAUUACCCGUtt	Transcription
46	POU5F1	83.011	194.043	5460	GGAGAUAUGCAAAGCAGAAtt	Transcription
47	POU5F1	85.820	180.401	5460	GUCCGAGUGUGGUUCUGUAtt	Transcription
48	RDBP	97.298	183.386	7936	AGAGGACCCAGAUUGUCUAtt	Transcription
49	RDBP	111.487	145.707	7936	AAGUCAACAUAGCCCGAAAtt	Transcription
50	TBX1	75.599	193.846	6899	GCAAAGAUAGCGAGAAAUAtt	Transcription
51	TBX1	91.538	161.634	6899	GGAUCACGCAGCUCAAGAUtt	Transcription
52	ZBTB41	85.750	176.019	360023	CCAGUUCGACCUGAACAAAtt	Transcription
53	ZBTB41	83.351	171.308	360023	GACCUAUACUCAUUCUGCAtt	Transcription
54	ZNF358	61.490	256.085	140467	GUUUCGACCUCGAUCCAGAtt	Transcription
55	ZNF358	85.866	167.413	140467	CAGCCUCACCAAGCACAAAtt	Transcription
56	ABCB8	57.472	294.800	11194	CGACCAUCAUGGAAAACAUtt	Metabolic process
57	ABCB8	103.662	146.993	11194	CGCUUUAACUGGAAGCUCUtt	Metabolic process
58	ACSF2	59.084	288.857	80221	GAAACUGCAUGAGAAGACAtt	Metabolic process
59	ACSF2	80.013	234.608	80221	CGAUGUUCGUGGGACAUUCUtt	Metabolic process
60	ALDH3A2	87.831	171.072	224	CACUUUCCUGGGUAUUGUAtt	Metabolic process
61	ALDH3A2	115.513	141.760	224	CAACAGUACUUACCGAUGUtt	Metabolic process
62	OAZ1	94.839	169.972	4946	GCCUUGCUCCGAACCUUCAtt	Metabolic process
63	OAZ1	101.904	141.842	4946	GAUUAUCCUUGUACUUUGAtt	Metabolic process
64	PPP2R1A	60.645	254.007	5518	GAACAGCUGGGAACCUUCAtt	Metabolic process
65	PPP2R1A	104.020	161.613	5518	CUUCGACAGUACUUCCGGAtt	Metabolic process
66	PPP2R1A	96.357	157.243	5518	GGAGUUCUUUGAUGAGAAAtt	Metabolic process
67	4-Sep	68.989	220.902	5414	GGACCAAGCCCUAAAGGAAtt	Metabolic process

No.	Symbol	Viable cell density (%)	per cell luciferase yield (%)	Gene_ID	siRNA sequence	Biological process
68	4-Sep	110.815	140.658	5414	GCAGUGGACAUAGAAGAGAtt	Metabolic process
69	DENND5B	76.131	235.013	160518	CGAUAUGCUUUUCUACGUUtt	Cation transport
70	DENND5B	83.636	176.821	160518	CCAGCGAUACAACUCCUAUtt	Cation transport
71	KCNJ10	83.512	259.478	3766	GCAGGCACAUGGUUCCUCUtt	Cation transport
72	KCNJ10	105.029	161.785	3766	AGGUCAAUGUGACUUUCCAtt	Cation transport
73	KCTD15	76.798	186.195	79047	CCAAGUCCAAUGCACCUGUtt	Cation transport
74	KCTD15	88.009	174.946	79047	CCUGGACAGUUUGAAGCAAtt	Cation transport
75	SLC12A8	78.156	185.175	84561	GCUUCCUCUUGGACCUCAAtt	Cation transport
76	SLC12A8	80.173	184.608	84561	GCGGAAAAGGUAUCCCUCAtt	Cation transport
77	CASP8AP2	67.320	284.062	9994	CCAACAAGGAAGACGAAAAtt	Apoptotic process
78	CASP8AP2	79.253	272.683	9994	CCCUGUUCAUUAUAAGUCUtt	Apoptotic process
79	CASP8AP2	89.677	157.868	9994	GGAUAUUGGAGGCUAGUCAtt	Apoptotic process
80	CDCA7	82.689	209.398	83879	GACUAUUGAUACCAAAACAtt	Apoptotic process
81	CDCA7	90.976	189.252	83879	GCAAUGCUUGCAAAACUCAtt	Apoptotic process
82	CCT2	85.046	189.850	10576	CAUUGGUGUUGACAAUCCAtt	Protein folding
83	CCT2	79.093	186.786	10576	GUUGCAAACUUAUCGAGGAtt	Protein folding
84	CCT2	91.558	160.246	10576	CUCUUAUGGUAACCAAUGAtt	Protein folding
85	CCT7	76.280	200.322	10574	AAAUGCAACCCAAAAAGUAtt	Protein folding
86	CCT7	90.987	160.687	10574	GUACCUGCGGGAUUACUCAtt	Protein folding
87	C22orf26	93.181	185.763	55267	CCACCCUACUAUGUACUGUtt	Miscellaneous
88	C22orf26	94.537	155.385	55267	GCUAAGUCUUUUUCCACAGUtt	Miscellaneous
89	C3orf19	91.714	202.960	51244	CAGUUACUUUCAAAACUCUtt	Miscellaneous
90	C3orf19	92.429	156.418	51244	CAACAGAUCAGAGAACAAAtt	Miscellaneous
91	CHAF1A	82.390	228.483	10036	GCCUGAAUCUUGUCCCAAAtt	Miscellaneous
92	CHAF1A	66.511	215.853	10036	GAAGAAGACUCUGUACUCAtt	Miscellaneous
93	CHAF1A	104.553	179.207	10036	CGAAACUUGUCAACGGGAAtt	Miscellaneous
94	EEF1B2	75.570	200.070	1933	AGAAAGCUUUGGGCAAAUAtt	Miscellaneous
95	EEF1B2	85.471	183.071	1933	GGAAGAACGUCUUGCACAAtt	Miscellaneous
96	EEFSEC	101.897	162.677	60678	GAACAAAAUAGACCUCUUAtt	Miscellaneous
97	EEFSEC	95.368	152.850	60678	CUGUGGAAAAGAUACCGUAtt	Miscellaneous

No.	Symbol	Viable cell density (%)	per cell luciferase yield (%)	Gene_ID	siRNA sequence	Biological process
98	FAM102A	66.121	214.156	399665	GCCCACUAUUCUCAGCUCAtt	Miscellaneous
99	FAM102A	105.514	143.889	399665	GCAUCUGUCCGAUCGCUCUtt	Miscellaneous
100	FRZB	74.811	205.132	2487	GGGACACUGUCAACCUCUAtt	Miscellaneous
101	FRZB	89.583	163.431	2487	CAUCAAGCCCUGUAAGUCUtt	Miscellaneous
102	ICA1L	67.947	258.104	130026	UGAAGAUAAUCGAGAAAUAtt	Miscellaneous
103	ICA1L	100.201	153.426	130026	ACAGGUCUUUAUCAAAGCAtt	Miscellaneous
104	MARK2	95.471	162.372	2011	GACUCAGAGUAACAACGCAtt	Miscellaneous
105	MARK2	112.248	137.554	2011	GCCUAGGAGUUAUCCUCUAtt	Miscellaneous
106	MFRP	88.359	164.639	83552	CUAACUACCCAGACCCUUAtt	Miscellaneous
107	MFRP	105.583	154.286	83552	GCAACAGAAUCGAGCAAGAtt	Miscellaneous
108	MGRN1	63.690	273.535	23295	CCCUGAAGGUUACCUCUUUtt	Miscellaneous
109	MGRN1	113.437	140.103	23295	GGAUGACGAGCUGAACUUUtt	Miscellaneous
110	OCRL	123.199	150.843	4952	GAUUACUUCUUGACUAUCAtt	Miscellaneous
111	OCRL	109.377	136.174	4952	CUCCCGCAGUUGAACAUCAtt	Miscellaneous
112	OR10P1	61.943	281.113	121130	CUCUGAUUGUCACCUCUUAtt	Miscellaneous
113	OR10P1	91.526	179.268	121130	GCUCCUCUGUUACCACAGAtt	Miscellaneous
114	PRR15	102.629	146.756	222171	CGCUCACCAACAGCAGAAAtt	Miscellaneous
115	PRR15	110.986	133.601	222171	CUUUUAAUGUUAAACUACAtt	Miscellaneous
116	RAB31	84.418	228.634	11031	GAACUUCACAAGUUCCUCAtt	Miscellaneous
117	RAB31	89.607	180.764	11031	CAAUGGAACAAUCAAAGUUtt	Miscellaneous
118	TACC2	82.634	188.258	10579	GGAUUACAGAAACUCCUAUtt	Miscellaneous
119	TACC2	108.211	141.104	10579	GAGCAGAGAUCAUAACCAAtt	Miscellaneous